# Two-electron QED contributions to the ground-state binding energy in He-like $Kr^{34+}$ ions

P. H. Mokler,[1] J. R. Crespo López-Urrutia,[1] F. J. Currell,[2,3] N. Nakamura,[3] S. Ohtani,[3] C. J. Osborne,[1] H. Tawara,[1] J. Ullrich,[1] and H. Watanabe[3]

[1]*MPI für Kernphysik, Saupfercheckweg 1, 69117 Heidelberg, Germany*

[2]*School of Mathematics and Physics, Queen's University, Belfast BT7 1NN, Northern Ireland, United Kingdom*

[3]*Institute of Laser Science, University of Electro-Communications, Chofu, Tokyo 182-0021, Japan*

(Received 19 October 2007; published 17 January 2008)

The two-electron QED contributions to the ground-state binding energy of $Kr^{34+}$ ions have been determined in two independent experiments performed with electron beam ion traps (EBIT) in Heidelberg (HD) and Tokyo (BT, Belfast-Tokyo collaboration). X rays arising from radiative recombination (RR) of free electrons to the ground state of initially bare $Kr^{36+}$ and hydrogenlike $Kr^{35+}$ ions were observed as a function of the interacting electron energy. The *K* edge absorption by thin Eu and W foils provided fixed photon energy references used to measure the difference in binding energy $\Delta E_{2e}$ between the H- and He-like Kr ions ($Kr^{35+}$ and $Kr^{34+}$, respectively). The two values agree well, yielding a final result of $\Delta E_{2e}=641.8\pm1.7$ eV, confirming recent results of rigorous QED calculations. This accuracy is just of the order required to access screened radiative QED contributions.

DOI: 10.1103/PhysRevA.77.012506 PACS number(s): 32.30.Rj, 32.10.−f, 31.30.J−

## I. INTRODUCTION

Electron-electron interactions play an essential role in the atomic structure of atoms and highly charged heavy ions with more than one bound electron [1,2]. Though one electron, i.e., hydrogenic, ions are well understood nowadays, see Refs. [3,4], the theoretical description of two-electron systems, the He atom and ions belonging to its isoelectronic sequence, is still far off from being complete. These species offer one of the most straightforward means for studying the bound state electron-electron interactions in different regimes. The ratio of its strength versus that of the electron-nucleus interaction can be varied along the isoelectronic sequence over a wide range. At high values of the atomic number *Z*, QED effects—scaling for the most important one loop terms with approximately $Z^4$—make increasingly larger contributions to the binding energy and become essential for its quantitative understanding. At the same time, the growth of the QED terms over many orders of magnitude allows one to experimentally test the sophisticated methods used to calculate such contributions as they become too large to be treated perturbatively. This field of nonperturbative, high-field bound state QED has remained very active in the last years. Relatively recent reviews of theoretical and experimental achievements can be found in, e.g., Refs. [5,6].

Since the first systematic theoretical analysis of the Lamb shift for the ground state ($n=1$) in He-like ions using series expansions up to orders of $\alpha(\alpha Z)^4$ and $\alpha^2(\alpha Z)^3$ (with $\alpha$ the fine structure constant and *Z* the atomic number) were reported [7,8], a number of high-order QED corrections have been calculated over a wide range of atomic numbers *Z* [9–13]. The most recent summary has been given by Artemyev *et al.* [14]. In contrast to this state of the theoretical studies, experimental data for the two-electron contributions to the ground state in He-like ions are very scarce and also not sufficiently accurate for a detailed test of those predictions [15].

Thus far, in most cases the two-electron contributions to the ground state in heavy He-like ions including QED and other effects have been determined through high accuracy x-ray spectroscopy (at the level of tens of ppm) of the $K\alpha$ transition energies. These studies relied on the assumption that the energies of the excited states can be calculated precisely enough [16]. However, $K\alpha$ x-ray transitions from different initial states (of the same shell; $n=2\rightarrow n=1$) cannot be fully resolved for heavy ions with present day spectrometers. This is especially true if the electronic structure of the ion is disturbed by the presence of additional, loosely bound so-called "spectator electrons," which give rise to energy variations of the electronic states and hence to spectral lines' shifts, and to the appearance of satellite transitions. In plasmas with very high excitation or recombination rates, multiply excited states relax through such transitions, which in many cases cannot be fully resolved from the unshifted original line and thus affect the experimental results. Moreover, as the dominant contributions to the binding energies in He-like ions originate from the one-electron parts—as also seen in H-like ions—a comparison of x-ray transitions within such He- and H-like ion species always tends to be accompanied by systematic uncertainties [17].

Therefore, it would be obviously better to measure the ionization energies of the ground states (*K* shell) of "pure" He-like ions (such without any spectator electrons) and compare them with the corresponding values for H-like ions. In this way, ambiguities related to the calculation of the energies of excited states would be eliminated. Moreover, in such a differential comparison of ionization energies between H- and He-like ions, nuclear effects such as size and charge distribution cancel almost completely. In particular, the various correction terms originating from the one-electron part vanish to high order. Thus, the true two-electron contributions to the binding energies in He-like systems are clearly isolated from the one-electron parts. Furthermore, such a differential measuring technique does not demand a precise absolute energy determination, since only an accurate energy difference has to be determined. This doubly differential technique—differential in experimental and theoretical values—yields much higher accuracy and more confidence

 

in the comparison between experiments and theory, as most correction terms on both sides cancel.

The first differential measurements of such a kind were reported already in 1982 by observing x rays from radiative electron capture (REC) into fast bare and H-like ions—specifically $F^{9+}$ and $F^{8+}$ ions [18]. The REC of quasifree electrons to the projectile $K$ shell was measured as a function of the ion kinetic energy and extrapolated to zero energy for determination of the binding energies. Radiative recombination (RR [19], see below) and REC are similar processes, with the difference that the electrons to be captured are either free or only "quasifree" (i.e., softly bound to a light target atom), respectively. Due to the Compton profile, i.e., the momentum distribution of the "quasifree" electrons, however, the REC transitions are much broader than genuine RR lines, leading to large uncertainties in the final results, and thus preventing a detailed comparison of fast-beam REC results with theory. Hence, further REC studies did not really aim towards the field considered here, see Ref. [20], and references cited therein.

The basic idea of the doubly differential measurement technique has recently been utilized to study x rays from RR into initially bare and H-like heavy ions either produced in an electron beam ion trap (EBIT) [21,22] or stored in the heavy ion storage ring ESR [23]. In RR a free electron is radiatively captured by an ion. The energy $E_{\mathrm{RR}}$ of the emitted photon corresponds to sum of the initial kinetic electron energy in the ion motional frame $E_e$ and the final electron binding energy $I_B$:

$$E_{\mathrm{RR}} = E_e + I_B. \tag{1}$$

Knowing the initial electron energy and measuring the x-ray energy of the emitted RR photon leads straight to the binding energy for the last bound electron. Hence, comparing x-ray energies from $K$-RR (RR to the $K$ shell) for initially bare and H-like heavy ions delivers directly the two-electron contribution $\Delta E_{2e}$ for He-like species in the ground state ($n=1$):

$$\Delta E_{2e}\ (\text{He-like ion}) = E_{K\text{-RR}}\ (\text{bare ion}) - E_{K\text{-RR}}\ (\text{H-like ion}). \tag{2}$$

The difference between the two experimental approaches is that in an EBIT the highly charged ions (HCI) are practically at rest and the electrons move at high velocity, whereas in an ion storage ring the ions circulate at high velocity and the electrons to be captured (usually taken from the storage ring's electron cooler) show with respect to the ions only a small velocity difference. In the ESR case the recombination x rays are emitted in the ion's velocity frame, and thus the Doppler effect has to be taken into account for the energy evaluation. In both the cases (EBIT and ESR) standard intrinsic Ge solid-state detectors have been generally used for energy determination of the x rays.

More recently, at the EBIT devices in Oxford and Tokyo a slightly different spectroscopy approach was taken to infer the two-electron contribution $\Delta E_{2e}$. Currell *et al.* used the absorption edge spectroscopy technique (dubbed absorptiometry) for the study of $Ar^{16+}$ [24,25]. The sudden intensity drop-off in the $K$-RR x-ray emission observed behind an absorber foil as the $K$ edge $E_A$ is crossed was utilized to determine the x-ray energy. In these experiments, the electron energy $E_e$ (and hence photon energy $E_{\mathrm{RR}}$) was gradually increased while the photon flux transmitted through the absorber foil was recorded. At an electron beam energy where the intensity suddenly drops, due to one of the RR peaks passing from an energy below the absorber's $K$ edge to an energy above this edge, the photon energy of that RR peak is known:

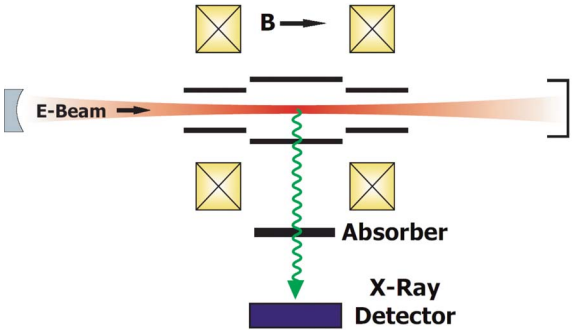


FIG. 1. (Color online) Absorptiometry at an EBIT. The central ion trap region is defined axially by the electrostatic potentials applied to the drift tubes (black) and radially by the negative space charge of the magnetically (B) compressed electron beam.

$$E_{K\text{-RR}} = E_A. \tag{3}$$

The drop-off in transmitted intensity appears at different electron energies for initially bare and H-like ions due to their different binding energies—cf. Eq. (1). This difference in the drop-off electron energies corresponds exactly to the two-electron contribution $\Delta E_{2e}$ of the He-like ions. The experimental resolution is not determined by the x-ray detector but by the natural width $\Delta E_A$ of the absorption edge and by the electron beam energy spread.

For the present work this absorptiometry technique has been employed independently at the EBITs in Heidelberg (HD) [26] and Tokyo (BT—in collaboration with Belfast) [27] to determine the two-electron contribution $\Delta E_{2e}$ for the ground state in He-like $Kr^{34+}$. In both cases $Kr^{35+}$ and $Kr^{36+}$ were produced and stored under different conditions especially concerning the electron energy range used. $K$-RR x rays to the initially bare and H-like ions were measured by Ge(i) detectors using an appropriate absorber. The difference in the drop off energies yields a value for $\Delta E_{2e}$. Both concurring results are compared to the most recent available predictions [14].

## II. EXPERIMENTS

The principle of the present absorptiometry measurements at EBIT is sketched in Fig. 1. In such a device, an energetic electron beam compressed by a strong magnetic field B ionizes successively the ions to high charge states. The produced HCIs are confined in the central trap region radially by the space charge potential of the electron beam and the Lorentz force due to the magnetic field and axially by electrostatic potentials applied to the drift tubes surrounding the

TABLE I. Operating parameters used at the two EBITS for the present experiments.

| EBIT | Heidelberg (HD) | Tokyo (BT) |
|---|---|---|
| Electron beam energy range $E_e$ (keV) | $32.5 \pm 1.0$ | $51.0 \pm 0.9$ |
| Electron beam energy width $\Delta E_e$ (eV) | 40 | 100 |
| Bare to H-like ion abundances, ratio (%) | 20 | 40 |
| Absorber (and thickness) | $_{63}$Eu (100 ($\mu$m)) | $_{74}$W (100 ($\mu$m)) |
| K edge of absorber $E_A$ (keV) [31] | 48.5190 | 69.5250 |
| K edge width $\Delta E_A$ (eV) | $\approx$16 | $\approx$38 |
| Ge(i) detector size (mm$^2$) | 1000 | 2800 |
| Electron current (mA) | 220 | 150 |
| Scan channel width ($\Delta$V/channel) | 1.317 | 0.489 |
| Slew rate (V/s) | 3 | 40 |

trap region. The electron density reaches values of $10^{11}-10^{13}$ $e/\mathrm{cm}^3$, the ion density is about two orders of magnitude smaller. In this environment, the monoenergetic electron beam generates a narrow charge state distribution, in which the ions are excited frequently by electron impact but dwell most of the time in their electronic ground state due to fast radiative and nonradiative relaxation processes [28].

With a certain probability, trapped HCIs may also recombine radiatively (RR) with electrons from the ionizing electron beam. The x rays emitted by this process are monitored perpendicularly to the beam axis. They exit the vacuum chamber through a thin Be observation window and pass subsequently through an absorber foil, before they are registered by a Ge detector. Their intensity and energy are recorded as a function of the acceleration potential applied to the electron beam. An intensity drop-off is the signature when the rising $K$-RR photon energy reaches a certain value corresponding to the $K$-edge absorption energy of the material chosen [see Eq. (3)].

As the experimental procedures at both EBIT laboratories are to a large extent similar, we exemplify below the principle by describing the HD measurements, and emphasize particularities of the BT method only wherever needed. The main difference between both experiments is the electron energy $E_e$ applied to produce the required highly charged Kr ions in the trap. This has two important consequences. (i) The materials of the absorber foils used are not the same, as their $K$-edge energies $E_A$ have to match the $K$-RR x-ray energies [$E_{K\text{-RR}}$, see Eq. (1)]. (ii) The abundances for bare and H-like ions are different. Moreover, the magnetic field, the electron beam current, the trap depth, the energy scan width (channel resolution), and its slew rate (scan velocity) were different at the two devices. The main parameters are summarized in Table I.

The HD-EBIT [26] was operated at electron beam energies $E_e$ of 31.5–33.5 keV and a nominal current of 220 mA. The central magnetic field strength in the cryogenic device was 8 T. The Kr pressure at the first (of four) differential pumping stage of the gas injector used to feed an Kr atomic beam to the trap was $1\times10^{-7}$ mbar. The acceleration potential was varied with a slow scanning rate of 3 V/s in order to minimize dragging in the voltage reading as well as perturbations in ion charge balance. At the ramp end for each scan (which lasted about 700 s) the ions accumulated in the trap were dumped by applying an appropriate voltage pulse to the drift tubes. For a detailed description of these procedures and the data acquisition setup we refer to the work by González Martínez *et al.* [29]. Under these operating parameters, the charge state balance in the trap remains in steady state conditions. Thus, the abundance ratio between the charge states is determined mainly by the cross sections for electron impact ionization and radiative recombination at the instantaneous electron beam energy, and the residual gas pressure in the trap region, which induces ion recombination through charge-exchange collisions. At the HD EBIT the ratio of $Kr^{36+}$:$Kr^{35+}$ ion population was estimated from the RR line intensities to be $\sim$0.2. The question arises about the possible population of multiply excited states under these conditions. It should be emphasized that even if double or multiple electron capture to high-lying ion states by these mechanisms would occur, these levels would relax to the ground state by fast radiative decay channels. Nonradiative decay channels, as well as reionization of long-lived multiply excited states (which have large geometrical cross sections) also quickly deplete high lying levels. In other words, the ionization, excitation and charge-exchange collision rates are in an EBIT much slower than the deexcitation rate. This implies that the ions trapped remain most of the time in their electronic ground state. Hence, energy shifts due to spectator electrons do not have to be considered for the observed transitions.

### A. Electron energy determination

In order to precisely determine the actual electron interaction energy $E_e$ all the applied voltages as well as the space charge potentials generated by the electron beam and the trapped ions have to be considered. Thus,

$$E_e = e(V_C + V_G + V_D - V_{\mathrm{SC}}^e + V_{\mathrm{SC}}^i), \tag{4}$$

where $V_C$ is the constant cathode voltage (1.500 kV), $V_G$ the (constant) voltage of the electron gun platform (here 20 kV), $V_D$ the (ramping) drift tube voltage, the space charge potentials $V_{\mathrm{SC}}^e$ and $V_{\mathrm{SC}}^i$ caused by the primary electron beam and the accumulated positive ions, respectively. The fraction $\varepsilon_{\mathrm{SC}}=V_{\mathrm{SC}}^i/V_{\mathrm{SC}}^e$ gives the compensation of the electron space charge by the space charge brought into the trap by the ac-

cumulated HCIs. As generally the ions are confined very closely along the axis near the trap centre, the effects of other potentials appearing along the electron beam axis but outside the central trap region are negligible. However, the radial space charge distribution influences significantly the electron energy and also determines the width of electron beam energy distribution. This leads to a broadening of the RR x-ray lines. But this effect similarly acts on both ion species and does not influence the difference in the drop-off energies. The estimated widths for the electron energy distribution $\Delta E_e$ are given in Table I.

### B. Acceleration voltage measurement

Special care has been taken for an accurate stabilization of the voltages, their precise calibration and exact reading. At the HD EBIT special, highly stabilized voltage dividers were developed [30]. The precision voltage dividers were calibrated at the German National Standard Institution (PTB) and showed negligible nonlinearities of less than a few ppm over the narrow range of voltages used in the present work. In order to avoid any drifts during measurements, the temperature variation in the laboratory was kept below $\pm 0.3\ ^\circ\mathrm{C/h}$ and the temperature inside the divider boxes was kept constant within $\pm 0.04\ ^\circ\mathrm{C}$. The final voltage variations originate from small instabilities in the power supplies (not additionally temperature stabilized) in the region of $10^{-4}/^\circ\mathrm{C}$ totaling up to about 0.7 V. The high-frequency RMS voltage ripple ($V_{\mathrm{rip}}=1.7$ V) contributes to a broadening of the electron energy distribution (as the voltage divider integrates with a time constant longer than the ripple period). However, this contribution does not affect the average electron energy and hence the precision of this experiment.

### C. Space charge potentials

If the electron beam current is kept constant, the electron space charge potential varies with the electron energy $E_e$, as it essentially follows the electron beam density. We take into account the actual space charge potential variation due to this effect at the specific *K*-edge energies appearing for the different cases, *K*-RR for initially H-like and bare Kr ions $V_{\mathrm{SC}}^{e}(\mathrm{Kr}^{35+})$ and $V_{\mathrm{SC}}^{e}(\mathrm{Kr}^{36+})$, respectively. For an electron beam with 32 keV and 220 mA, the space charge potential $V_{\mathrm{SC}}^{e}$ is calculated to be 122 V, and with a space charge compensation of $\varepsilon_{\mathrm{SC}}=40\%$ we yield correspondingly $V_{\mathrm{SC}}^{i}=48.4$ V [30]. For this difference in the total space charge potentials we determine a correction of $\Delta V_{\mathrm{SC}}=+0.7$ V between $\mathrm{Kr}^{35+}$ and $\mathrm{Kr}^{36+}$ (at $E_e=32.65$ and 32.00 keV, respectively) at the electron beam current value of 220 mA. This correction has to be included in the final electron energy difference. In this regard we note that the radial density distribution of the electron beam causes slight radial energy deviations within the beam radius. However, the possible contribution from this effect is minimized as both ion species, $\mathrm{Kr}^{35+}$ and $\mathrm{Kr}^{36+}$, display nearly the same spatial distribution inside the electron beam as their $q/m$ ratios are very close to each other.

### D. X-ray absorption

Generally, the edge energy of an absorber material $E_A$ is defined as the ionization (threshold) energy $I_B$ (of an electron in a particular shell). For *K*-shell ionization in Eu we have $E_A=48.5190$ keV [31]. However, the real x-ray absorption profile is known to be shifted downwards from the threshold energy by a few eV compared to the tabulated values; this is due to contributions from excitation to high-lying vacant states, resulting in asymmetric profiles in most cases [32]. Such detailed profiles are only known for a few elements in the gas phase but not for actual solid absorber foils. Here, beyond excitation to high-lying states additional solid state effects have to be taken into account to explain the actual absorption profile. In fact only specific and detailed measurements, e.g., using synchrotron radiation can solve this experimental difficulty. For an estimate of the absorber widths the lifetime of the produced vacancy state can give a reasonable guideline and literature values may be used, see Ref. [31]. For heavy absorbers (with atomic number $Z_A$) the width for the *K* edge is mainly determined by the $K\alpha$ decay rates and increases roughly with $Z_A^4$, see, e.g., overview in Ref. [33]. For *K* edges typical widths between 40 and 80 eV have been cited for $66 \leqslant Z_A \leqslant 82$ [34]. However, neither the exact absolute edge energy of the absorber nor its accurate width is crucial for the present type of differential measurement; here only the difference in the energies, where a sudden steplike reduction in intensity is observed, is decisive—recall these steplike reductions are due to the energies of photons from *K*-RR into initially $\mathrm{Kr}^{35+}$ and $\mathrm{Kr}^{36+}$ ions becoming greater than the absorption edge energy. Any subtle peculiarities of the absorption profiles are not at all critical, as they will have the same effect on the observed intensity edges for the two charge states and hence any such effect will cancel from the final analysis. In the present experiment, a 100 $\mu$m thick $_{63}$Eu foil was used which absorbs about 65% of the x rays beyond the edge and thus yields a noticeable intensity drop-off [35].

### E. X-ray detection

An ultrapure Ge detector (ORTEC GLP series) with a 13 mm thick and 36 mm diameter Ge crystal with a 250 $\mu$m thick Be window was positioned behind the Eu absorber foil. The EBIT x-ray vacuum window is also made of a 250 $\mu$m thick Be foil. Two additional 25 $\mu$m thin Be windows are attached to each of the two thermal shields surrounding the superconducting magnet inside the vacuum chamber adding to a total Be thickness of 550 $\mu$m. The detector was carefully and repeatedly calibrated between 40 and 122 keV by using characteristic *K*-x rays from Eu, Ta and Pb induced in foils of those materials through $^{57}$Co (122 keV) $\gamma$-ray irradiation. The resolution of the detector of about 550 eV FWHM is not crucial for the experiment, as in the end the actual energy resolution is mainly determined by the width of the absorber edge. Similarly, an accurate absolute energy calibration is not really essential for the differential measurement. However, the measured width of the intensity drop-off is finally not exclusively determined by the narrow absorber edge width but also by the spread of the electron beam energy distribution (see the values on Table I).

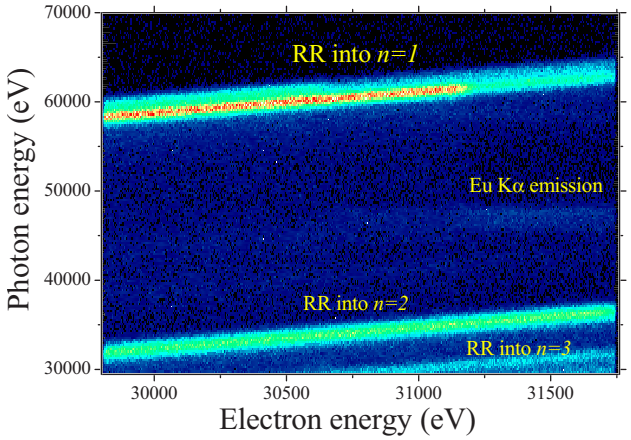


FIG. 2. (Color online) Two-dimensional plot of the radiative recombination (RR) photon yield into the different principal quantum number $n$ open shells as transmitted through an Eu absorber foil. Color-coded x-ray photon intensity versus electron energy $E_e$ and x-ray energy $E_X$. Faint decreases of the x-ray intensity of the RR into $n=1$ at approximately 30 700 and 31 300 eV electron beam energy indicate that the RR photon energy for the $Kr^{36+}$ and $Kr^{35+}$ ions, respectively, have reached the Eu $K$-shell absorption edge.

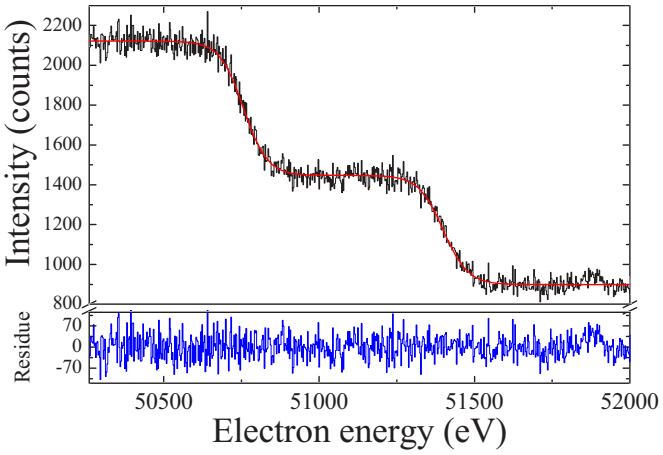


FIG. 3. (Color online) Integrated $K$-RR x-ray intensity projected onto the electron energy axis (BT experiment). The curve is fitted according to Eq. (5). The left and right steps are caused by $K$-RR to initially bare and H-like ions, respectively. The bottom graph shows the fit residuals.

### F. X-ray emission

The observed x-ray flux behind the Eu absorber is illustrated by the 2D intensity plot in Fig. 2. The color coded x-ray intensity is shown in the plane defined by the x-ray energy $E_X$ (vertical axis) and the electron energy $E_e$ (horizontal axis). A projection of a narrow vertical cut around a fixed electron energy results in an x-ray spectrum under those conditions. The intensity decrease observed at fixed x-ray energy corresponds to the $K$-edge absorption of Eu [see Eq. (3)].

In the two-dimensional matrix obtained in this way the slanted feature (double ridge) appearing at high photon energies is due to the $K$-RR emission, both for initially H-like and bare Kr ions. For these recombination lines the x-ray energy increases equally with the electron energy [see Eq. (1)]. This feature is now projected onto the horizontal axis. In this way, the electron beam energy dependence of the $K$-RR photon flux transmitted through the Eu foil is obtained. The difference between the drop-off energies of both charge states corresponds directly to $\Delta E_{2e}$, the two-electron contribution of interest.

An additional feature in the plot is a very faint horizontal line occurring beyond the drop-off energies in the middle of the plot. It results from the characteristic K$\alpha$ fluorescence of the Eu foil induced by $K$-RR x rays with energies higher than the $K$ edge. At the lower part of the figure, the other slanted lines represent $L$-RR and $M$-RR, i.e., radiative recombination into the $L$ and $M$ shell, respectively.

The Tokyo EBIT [27] was operated at higher electron impact energy (see Table I). Hence, the $K$-RR energies are correspondingly higher [Eq. (1)]. A W foil ($Z=74$) was used as absorber. Two-dimensional intensity plots equivalent to that shown in Fig. 2 were obtained. The slanted $K$-RR double line—summed over both, the bare and H-like contributions—was projected onto the electron energy $E_e$ axis. The resulting intensity profile depicted in Fig. 3 displays the two drop-off edges of $K$-RR corresponding to initially bare and H-like Kr ions. The energy difference between them corresponds to the difference in binding energies of H- and He-like Kr ions $\Delta E_{2e}$, after taking into account the slight variation in space charge with $E_e$ as described above.

### G. Data analysis

The line in Fig. 3 gives a fit to the BT data using the sum of two error functions for the transmitted x-ray intensity in the depicted window:

$$I_x = A_o + A_1 \mathrm{Erf}\{(E_A - E_e)/\delta E_A\} + A_2 \mathrm{Erf}\{(E_A + \Delta E_{2e} - E_e)/\delta E_A\}. \quad (5)$$

Here $A_o$ represents a constant background while $A_1$ and $A_2$ represent the contributions of each step. $E_e$ is the electron energy, $E_A$ and $\delta E_A$ are the lowest-lying (into $Kr^{36+}$) absorption energy observed and its width, respectively. $\Delta E_{2e}$ is the two-electron contribution. By casting the fitting function in this form, the two-electron contribution and its statistical error are directly extracted from a single fit.

In the Heidelberg experiment the slanted double line was split into two separated cuts along the $K$-RR lines, corresponding to initially bare and H-like ions respectively. These cuts are shown in Fig. 4. The integrated intensity profiles along the two cuts are displayed in Fig. 5. In this case, the edges in the distributions have been analyzed using Boltzmann step functions

$$I_x = C_2 + (C_1 - C_2)/[1 + \exp\{(E_e - E_A)/\delta E_A\}]. \quad (6)$$

Here $C_1$ and $C_2$ represent the intensity $I_x$ in the flat parts on either side of an edge; $E_A$ and $\delta E_A$ are the absorber edge energy observed and its width as parameters, respectively. The lines represent the fits obtained using these functions, from which $\Delta E_{2e}$ is extracted.

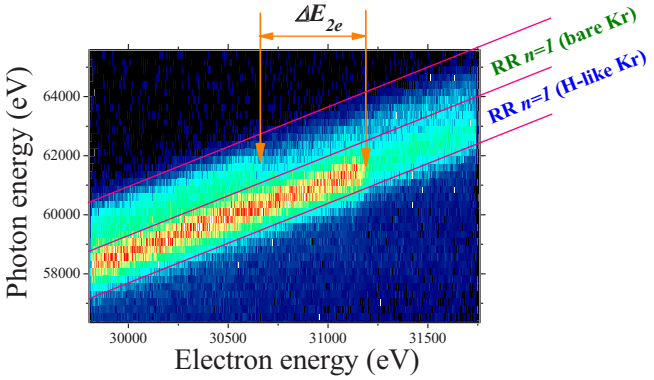


FIG. 4. (Color online) Detail view of the two-dimensional plot of the radiative recombination (RR) photon yield (x-ray photon energy $E_x$ versus electron energy $E_e$) in the HD experiment. Two cuts were made accordingly to select the RR emission of the initially bare and H-like ions.

### III. RESULTS AND DISCUSSION

The final values for the two-electron contribution, $\Delta E_{2e}$, from each of the experiments are

$$\Delta E_{2e} = 640.9 \pm 2.5 \text{ eV} \quad \text{(HD)}$$

and

$$\Delta E_{2e} = 642.8 \pm 2.2 \text{ eV} \quad \text{(BT)},$$

in close agreement with each other. The average value resulting from the two experiments is therefore:

$$\Delta E_{2e} = 641.8 \pm 1.7 \text{ eV}.$$

These results confirm also a preliminary value of $640.7 \pm 4.1$ eV published earlier by the Tokyo-Belfast collaboration [22]. Moreover, our results concur with the most advanced calculations of Artemyev *et al.* [14], which yield a value of

$$\Delta E_{2e} = 639.8162 \text{ eV}.$$

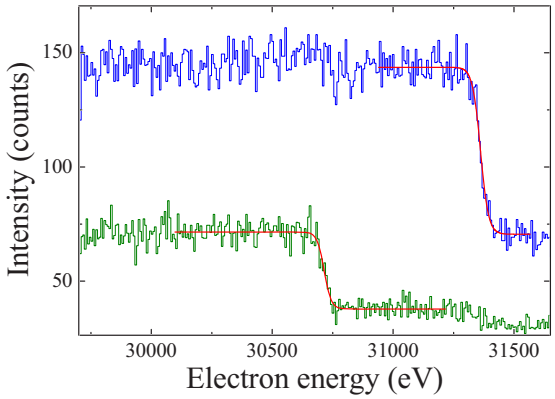


FIG. 5. (Color online) *K*-RR x-ray intensity projections along the electron energy axis (HD experiment) for the two cuts shown on Fig. 4 according to the initially bare (lower curve) and H-like (upper curve) ions. The lines are fits according to Eq. (6).

TABLE II. Contributions to the two-electron part of the binding energy $\Delta E_{2e}$ in $Kr^{34+}$ (in eV) according to Artemyev *et al.* [14].

| | |
|---|---|
| Coulomb term including all one-photon terms | 645.7802 |
| Nonradiative part of the two-photon exchange | −5.4737 |
| Screened QED part of the two-photon exchange | −0.5153 |
| Exchange terms by three and more photons | 0.0300 |
| Two-electron part of the recoil correction | −0.0034 |
| Higher order QED corrections | −0.0017 |
| Total value | 639.8162 |

These calculations, essentially an extension of the earlier work by Yerokhin *et al.* [13], are based on a rigorous QED treatment of the two-electron system including all two-photon terms and important three-photon contributions. The cited theoretical value contains the contributions from various effects shown in Table II.

For completeness we compare also our results with predictions by Indelicato *et al.* [9], Drake [10], Plante *et al.* [11] and Persson *et al.* [12]. They are listed in Table III together with the experimental values.

As can be read from Table III, the experimental accuracy still needs further improvements to allow for a more comprehensive test of theory. The same is true for all the ion systems in the region of neighboring $Z$ values. In Fig. 6 we compare the measured two-electron contributions and their uncertainties with the theoretical results from Artemyev *et al.* [14] along the isoelectronic He sequence. Beyond the present values (triangles at $Z=36$ for Kr), earlier results from the EBIT laboratories in Livermore ( [21]—squares for Ge, Xe, Dy, W, Os, and Bi) and Tokyo ( [22]—diamonds for Kr and Rh; [25]—triangles at $Z=18$ for Ar) and from the GSI heavy ion storage ring ESR ([23]—circles for U) are included. Except for the present Kr data and for Ar (both indicated by triangles), which were obtained applying the absorptiometry technique, conventional energy-dispersive solid-state detectors were used at the EBIT laboratories in Livermore (squares) and Tokyo (diamonds) as well as at the ESR (circles). In the present representation (see Fig. 6) the total

TABLE III. Comparison of available values for the two-electron contribution $\Delta E_{2e}$ in $Kr^{34+}$ (in eV). Theoretical values in italics were interpolated when needed with a $Z^3$ law. In the Drake result, the value for the corresponding H-like system calculated by Johnson and Soff [3] was subtracted.

| | | |
|---|---|---|
| *Theory* | Indelicato *et al.* 1987 [9] | *640.53* |
| | Drake 1988 [10] | 639.94 |
| | Plante *et al.* 1994 [11] | *640.76* |
| | Persson *et al.* 1996 [12] | *640.61* |
| | Yerokhin *et al.* 1997 [13] | *639.54* |
| | Artemyev *et al.* 2005 [14] | 639.8162 |
| *Experiment* | Nakamura *et al.* 2003 [22] | $640.7 \pm 4.1$ |
| | Heidelberg (*this work*) | $640.9 \pm 2.5$ |
| | Belfast-Tokyo collab. (*this work*) | $642.8 \pm 2.2$ |
| | final value (*this work*) | $641.8 \pm 1.7$ |

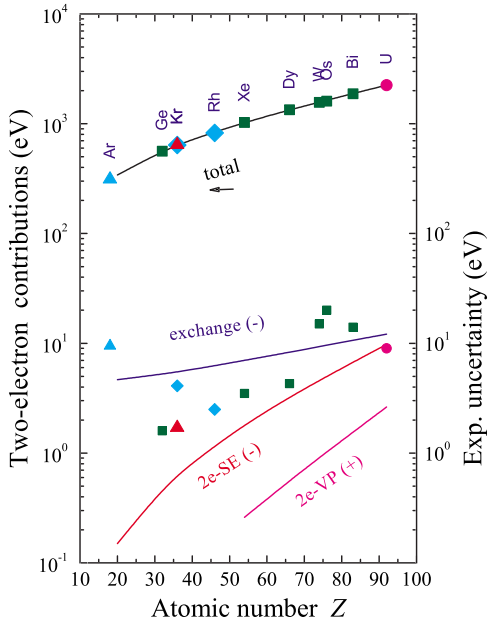


FIG. 6. (Color online) Experimental two-electron contributions $\Delta E_{2e}$ along the He-like isoelectronic sequence compared to rigorous QED calculations (continuous lines) of Artemyev *et al.* [14]. Present results: triangles at $Z=36$ (Kr). Earlier experimental data, LLNL-EBIT: squares (Ge, Xe, Dy, W, Os, Bi) [21], Tokyo-EBIT: diamonds (Kr, Rh) [22], and triangles on the far left (Ar) [25], GSI-ESR: circles (U) [23]. Top: total $\Delta E_{2e}$ values. Lower part: experimental uncertainties (same symbols) compared to the two-photon terms: exchange, screened self energy $2e$-SE, and screened vacuum polarization $2e$-VP.

values from the different experiments cannot be distinguished within their respective accuracies from the total theoretical values (upper part of the figure). In the lower part of the figure, the achieved experimental accuracies are compared to the pure two-photon exchange terms. All along the isoelectronic sequence the accuracies are better or at least comparable to these theoretical terms, therefore confirming those predictions. Moreover, for the most precise experiments the accuracy achieved just approaches the size of the hitherto not well studied "screened QED" terms, in particular the screened self-energy. Here, we may also infer accordance between theory and experiment.

Obviously, the accuracy of future experiments has to be further enhanced for more stringent tests of theory. The present method, the differential absorptiometry, can still certainly be improved considerably in the medium $Z$ region (around Kr). This is especially true if the EBITs are operated at relatively low electron currents to reduce the electron beam energy spread. Moreover, at the lower electron energies needed in this region, yielding also accordingly lower $K$-RR x-ray energies, the use of absorber materials of lower $Z$ elements is possible. These elements also offer narrower absorption edge widths. It would be worthwhile to investigate ion species with the highest possible $Z$ for any given absorber material to optimize the accuracy. In any case, uncertainties arising from counting statistics, background, voltage determination, and space charge contributions have to be reduced by adequate technical means, such as larger detectors, voltage stabilization, etc. In this regard, no essential difficulties to achieve an improvement by nearly an order of magnitude are foreseeable.

It is encouraging to see that the two measurements reported here using completely distinct apparatus and operating conditions as well as different analysis procedures have produced results agreeing very well within their respective error bars. This supports the assertion underpinning the method that the differential measurement technique leads to direct cancellation of the main systematic errors. For very heavy systems, unfortunately, the absorptiometry technique cannot be applied as no absorbers beyond uranium exist; here classical spectroscopy techniques have to be used. Beyond an improvement in the techniques based on solid state detectors and on better statistics of those measurements, higher resolution x-ray detectors such as crystal spectrometers, bolometers, or microcalorimeters may also bring a breakthrough for these He-like systems. In future, excited states for He-like species may also be calculated with an accuracy allowing one to use data from bound-bound transitions to study high field QED contributions. In this connection we refer to the recent comparison between H-like Cl and He-like Ar ions delivering the most precise experimental values using high-resolution crystal spectroscopy [36]. Currently, however, the recombination technique applied in this work still seems to be superior to the study of bound-bound transitions for determining the true (isolated) ground-state contributions. In any case, both for the medium heavy $Z$ region as well as for very heavy systems, a refined test of high order two-electron QED contributions seems quite feasible in the near future. Such tests are essential to aid in deepening of our understanding of the electromagnetic interactions mediated by exchange of virtual photons in the nonperturbative regime. Finally, we would like to emphasize that H-like, He-like, and Li-like species yield insight into the various aspects of high-field QED, i.e., they are differentially sensitive to them, see, e.g., Ref. [15]. All these simple ionic sequences have to be investigated with high accuracy to secure further progress in this field.

## ACKNOWLEDGMENTS

It is a pleasure to acknowledge the excellent cooperation with the theory group of V. M. Shabaev in St. Petersburg. In particular we are indebted to A.N. Artemyev providing us with his most recent calculations.

[1] P. J. Mohr, G. Plunien, and G. Soff, Phys. Rep. **293**, 227 (1998).
[2] V. M. Shabaev, Phys. Rep. **356**, 119 (2002).
[3] W. R. Johnson and G. Soff, At. Data Nucl. Data Tables **33**, 405 (1985).
[4] M. I. Eides, H. Grotch, and V. A. Shelyuto, Phys. Rep. **342**, 63 (2001).
[5] H. F. Beyer and V. P. Shevelko, *Atomic Physics with Heavy Ions* (Springer, Heidelberg, 1999).
[6] S. G. Karshenboim, F. S. Pavone, F. Bassani, and M. Inguscio, *The Hydrogen Atom, Precision Physics of Simple Atomic Systems* (Springer, Heidelberg, 2001).
[7] H. Araki, Prog. Theor. Phys. **17**, 619 (1957).
[8] J. Sucher, Phys. Rev. **109**, 1010 (1958).
[9] P. Indelicato, O. Gorceix, and J. P. Desclaux, J. Phys. B **20**, 651 (1987).
[10] G. W. Drake, Can. J. Phys. **66**, 586 (1988).
[11] D. R. Plante, W. R. Johnson, and J. Sapirstein, Phys. Rev. A **49**, 3519 (1994).
[12] H. Persson, S. Salomonson, P. Sunnergren, and I. Lindgren, Phys. Rev. Lett. **76**, 204 (1996).
[13] V. A. Yerokhin, A. N. Artemyev, and V. M. Shabaev, Phys. Lett. A **234**, 361 (1997).
[14] A. N. Artemyev, V. M. Shabaev, V. A. Yerokhin, G. Plunien, and G. Soff, Phys. Rev. A **71**, 062104 (2005).
[15] P. H. Mokler, Radiat. Phys. Chem. **75**, 1730 (2006).
[16] S. MacLaren, P. Beiersdorfer, D. A. Vogel, D. Knapp, R. E. Marrs, K. Wong, and R. Zasadzinski, Phys. Rev. A **45**, 329 (1992).
[17] H. F. Beyer, R. D. Deslattes, F. Folkmann, and R. E. Lavilla, J. Phys. B **18**, 207 (1985).
[18] H. Tawara, P. Richard, and K. Kawatsura, Phys. Rev. A **26**, 154 (1982).
[19] Y. Hahn, Rep. Prog. Phys. **60**, 691 (1997).
[20] G. Bednarz, A. Warczak, D. Sierpowski, Th. Stöhlker, S. Hagmann, F. Bosch, A. Gumberidze, C. Kozhuharov, D. Liesen, P. H. Mokler, X. Ma, and Z. Stachura, Hyperfine Interact. **146/147**, 29 (2003).
[21] R. E. Marrs, S. R. Elliott, and Th. Stöhlker, Phys. Rev. A **52**, 3577 (1995).
[22] N. Nakamura, T. Nakahara, and S. Ohtani, J. Phys. Soc. Jpn. **72**, 1650 (2003).
[23] A. Gumberidze, Th. Stöhlker, D. Banas, K. Beckert, P. Beller, H. F. Beyer, F. Bosch, X. Cai, S. Hagmann, C. Kozhuharov, D. Liesen, F. Nolden, X. Ma, P. H. Mokler, A. Orsic-Muthig, M. Steck, D. Sierpowski, S. Tashenov, A. Warczak, and Y. Zou, Phys. Rev. Lett. **92**, 203004 (2004).
[24] F. J. Currell, D. Kato, N. Nakamura, S. Ohtani, E. J. Sokell, H. Watanabe, and C. Yamada, Phys. Scr. **T80**, 154 (1999).
[25] F. J. Currell, J. Asada, T. V. Back, C. Z. Dong, H. S. Margolis, N. Nakamura, S. Ohtani, J. D. Silver, and H. Watanabe, J. Phys. B **33**, 727 (2000).
[26] J. R. Crespo López-Urrutia, A. Dorn, R. Moshammer, and J. Ullrich, Phys. Scr. **T80**, 502 (1999).
[27] F. J. Currell, J. Asada, K. Ishii, A. Minoh, K. Motahashi, N. Nakamura, K. Nishizawa, S. Ohtani, K. Okazaki, M. Sakurai, S. Tsurubuchi, and H. Watanabe, J. Phys. Soc. Jpn. **65**, 3186 (1996).
[28] *The Physics of Multiply and Highly Charged Ions*, edited by F. J. Currell (Kluwer, Dordrecht, 2003), Vol. 1.
[29] A. J. González Martínez, J. Braun, G. Brenner, H. Bruhns, J. R. Crespo López-Urrutia, A. Lapierre, V. Mironov, R. Soria Orts, H. Tawara, M. Trinczek, and J. Ullrich, Phys. Rev. Lett. **94**, 203201 (2005).
[30] A. J. González Martínez, J. R. Crespo López-Urrutia, J. Braun, G. Brenner, H. Bruhns, A. Lapierre, V. Mironov, R. Soria Orts, H. Tawara, M. Trinczek, J. Ullrich, A. N. Artemyev, Z. Harman, U. D. Jentschura, C. H. Keitel, J. H. Scofield, and I. I. Tupitsyn, Phys. Rev. A **73**, 052710 (2006).
[31] J. A. Bearden and A. F. Burr, Rev. Mod. Phys. **39**, 125 (1967).
[32] M. Breinig, M. H. Chen, G. E. Ice, F. Parente, B. Crasemann, and G. S. Brown, Phys. Rev. A **22**, 520 (1980).
[33] P. H. Mokler and F. Folkmann, in *Topics in Current Physics* (Springer, Heidelberg, 1978), Vol. 5, p. 201.
[34] A. Krämer, S. R. Elliott, R. E. Marrs, J. H. Scofield, and Th. Stöhlker, Hyperfine Interact. **115**, 215 (1998).
[35] J. H. Hubbell, H. A. Grimm, and I. Overbo, J. Phys. Chem. Ref. Data **9**, 1023 (1980).
[36] H. Bruhns, J. Braun, K. Kubiček, J. R. Crespo López-Urrutia, and J. Ullrich, Phys. Rev. Lett. **99**, 113001 (2007).